Multivariate Techniques for Specifying Tree-Growth and Climate Relationships and for Reconstructing Anomalies in Paleoclimate

HAROLD C. FRITTS,[1] TERENCE J. BLASING,[1] BRUCE P. HAYDEN[3] AND JOHN E. KUTZBACH[2]

(Manuscript received 23 February 1971)

ABSTRACT

Ring widths from trees on certain sites reflect climatic variation. Therefore, long time series derived from replicated and precisely dated ring-width chronologies may be utilized to extend climatic records into prehistoric times. Multivariate analyses of tree-ring chronologies from western North America are used to derive response functions from which one can ascertain what climatic information each ring-width chronology contains. In addition, multivariate analyses are utilized to calibrate a large number of ring-width chronologies of diverse response functions and from widely dispersed sites with a large number of regional climatic variables. A series of transfer functions is derived which allows estimates of anomalous climatic variation from tree-ring records. Reconstructions of anomalous variations in atmospheric circulation for portions of the Northern Hemisphere back to 1700 A.D. are obtained by applying the transfer functions to tree-ring data for time periods when ring data are available but climatic data are not.

1. Introduction

Most climatic and hydrologic records in western North America are relatively short and inadequate for assessing long-term climatic variations. The mean and variance of such records are biased by recent anomalous variations in climate such as occurred since 1900 A.D. (Lamb, 1969; Fritts, 1969b). Because of the recent settlement and low population of western North America, few long climatic records are available. Still less is known about climatic anomalies over the Pacific Ocean.

The rings of trees in certain sites from western North America provide a unique source of information on past variations of climate and other environmental factors which prevailed over North America and the adjoining oceans. Tree rings can be precisely dated (Stokes and Smiley, 1968), and their widths can be used to extend the climatic record back in time (Fritts, 1969b).

However, extraction of this climatic information from tree rings has been limited, until very recently, because techniques were inadequate to handle the large number of variables that must often be considered. In the past it has been necessary to select highly stratified samples of trees whose growth has been similarly limited by a relatively small number of environmental variables, such as low precipitation and high temperature (at the arid forest border) or by low temperature and a short growing season (at the arctic treeline) (Fritts, 1969a). Although considerable success in reconstructing climate has been achieved by such stratified sampling of trees (Fritts, 1965), old-aged trees on less extreme sites have not been utilized and much available environmental information has probably been lost.

Recent advances in multivariate analysis and the availability of modern, high-speed computers now make feasible the objective analysis of tree-ring data representing a great diversity of responses to the environment. Subtle variations in a variety of environmental relationships can be evaluated, and differences as well as similarities in the tree-growth response can be used to reconstruct variations in paleoclimate.

2. Dendrochronological developments

For many years dendrochronologists have claimed that ring widths from trees on arid or extremely cold sites are natural records of the variability in past climate. More recent investigations show that highly significant statistical relationships exist between growth of trees on arid sites and climatic data (Fritts, 1965, 1969a; Fritts *et al.*, 1965a) and that the statistical correlations are supported by reasonable cause and effect relationships (Fritts, 1969a, b). The model for the physiological relationships, which are involved in growth on arid sites, is shown in Figs. 1 and 2 and is discussed elsewhere by Fritts (1970).

In addition, a new technology has been developed in computer processing (Fritts, 1963; Fritts *et al.*, 1969) and in statistical analysis (Fritts, 1969a, b; Julian and Fritts, 1968). This has facilitated the efficient sampling

[1] Laboratory of Tree-Ring Research, The University of Arizona, Tucson.

[2] Center for Climatic Research, University of Wisconsin, Madison.

[3] Department of Environmental Science, University of Virginia, Charlottesville.

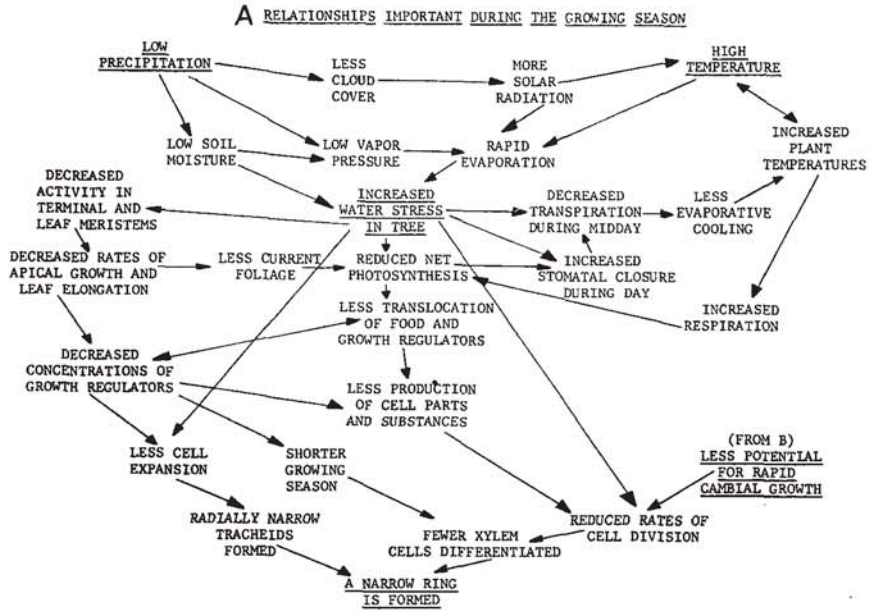

FIG. 1. Environmental and physiological relationships important during the growing season which will lead to the formation of a narrow ring in conifers growing on semi-arid sites.

and processing of tree-ring data and aided in the objective establishment of more than 200 new replicated tree-ring chronologies from western North America representing a large geographic area and diverse species and sites.

It is possible to select a highly stratified sample of drought-sensitive tree-ring chronologies distributed over a wide geographic area, and map and plot departures in growth as if they were actual occurrences of drought (Fritts, 1965). However, even in such a highly selected set of data there is some unexplained variability or "noise" because not all the sampled trees have identical responses to environmental factors.

In addition, there are many lengthy, well-dated ring-width chronologies containing highly significant information on climatic factors which are unusable in the above approach because growth was affected by factors other than drought during some portion of the year. For example, at certain times in the year, high precipitation and low temperatures may actually pro-

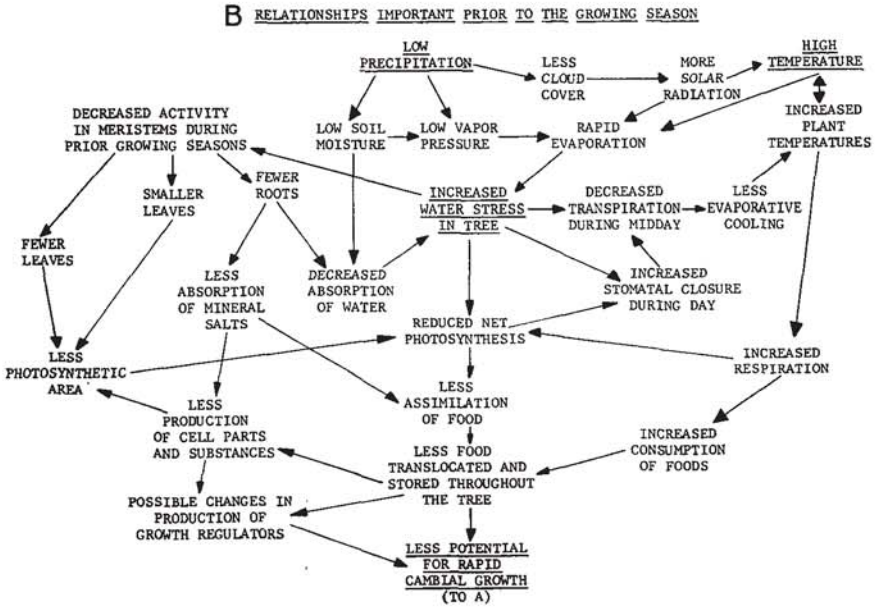

FIG. 2. Same as Fig. 1 except for relationships important prior to the growing season.

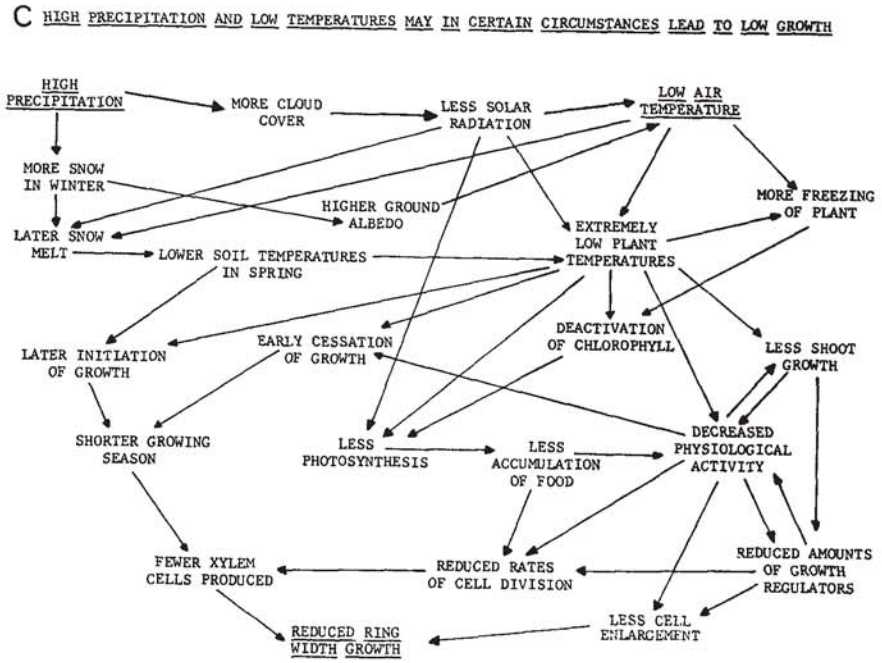

FIG. 3. Relationships that are opposite in effect from those shown in Figs. 1 and 2 which under certain circumstances may contribute to narrow rings.

duce conditions that ultimately limit subsequent growth. The explanations for many of these relationships are well reported in the physiological and ecological literature, and some of the relationships that are pertinent to the tree-ring samples are diagrammatically shown in Fig. 3. In general, as one proceeds northward from southwestern North America, or moves to higher elevations, the conditions shown in Fig. 3 become more and more important while those in Figs. 1 and 2 become less important.

Multivariate techniques provide a means of objectively defining how the ring-width growth relates to climatic factors at different periods during the growing season. They also provide a means of handling and relating two diverse data sets made up of many correlated variables.

3. Response functions relating tree growth to climate

In this section, response functions will be derived which relate ring-width chronologies to chronologies of the seasonal march of climate. Climatic data were taken from the decennial census of the United States climate. Each datum was a monthly average for a state climatic division (U. S. Weather Bureau, 1961, 1962, 1963). A total of 28 climatic regions were selected distributed over the western mountain states. Each region either included or was near one or more sites from which the tree rings were sampled. Monthly mean temperatures and total precipitation for a given July and the thirteen preceding months through June of the previous year were chosen as the 28 climatic variables from each region. Thirty-one observations of each of the 28 variables were utilized including data for 1931–62. All 31 observations were used to compute the mean and variance of each variable at each region to remove the average conditions of the region but preserve the climatic anomalies. The regions were then pooled, forming an array of 28 variables with 868 observations (28 regions×31 observations per region per variable), here denoted as ${}_m\mathbf{F}_n$, where the subscripts preceding and following the matrix symbol indicate respectively the number of rows and columns in the matrix. In this case, $m=28$, $n=868$. The pooling of regions provides stability and saves computational time. However, separate analyses of each climatic region or of specific climatic stations provide results that are comparable.

These normalized data were subjected to routine principal component analysis as follows:

$$ {}_m\mathbf{C}_m\mathbf{E}_m = {}_m\mathbf{E}_m\mathbf{L}_m, \quad m=28, \tag{1}$$

where

$$ {}_m\mathbf{C}_m = \binom{1}{n}{}_m\mathbf{F}_n\mathbf{F}_{m'}, \quad m=28, \quad n=868 \tag{2}$$

is the correlation matrix of the 28 climatic variables, ${}_m\mathbf{L}_m$ the (diagonal) matrix of eigenvalues, and ${}_m\mathbf{E}_m$ the complete eigenvector matrix corresponding to the eigenvalues $\mathbf{L}_i$, $i=1, m$. The p most important orthogonal eigenvectors are selected from the eigenvector matrix and represent p ways that temperature and precipitation may co-vary throughout the year.

The amplitudes, or multipliers, of these orthogonal eigenvectors, denoted ${}_p\mathbf{X}_n$, are then obtained:

$$ {}_p\mathbf{X}_n = {}_p\mathbf{E}_m'\mathbf{F}_n, \quad m=28, \quad n=868, \tag{3} $$

where the original 28 climatic variables representing the seasonal march of climate are now expressed in terms of a smaller array p, $p<28$. In the analyses reported here, $p=20$, and these 20 variables account for 95% of the total variance. Stepwise multiple regression is used to estimate a ring-width chronology within or near a climatic region, ${}_1\mathbf{P}_n$, from the amplitudes representing the climatic variables for that region

$$ {}_1\hat{\mathbf{P}}_n = {}_1\mathbf{R}_p\mathbf{X}_n, \quad n=31, \tag{4} $$

where ${}_1\mathbf{R}_p$ is a row vector of significant regression coefficients (all insignificant ones are assigned a value of zero). Substituting Eq. (3) into (4), we have

$$ {}_1\hat{\mathbf{P}}_n = {}_1\mathbf{R}_p\mathbf{E}_m'\mathbf{F}_n = {}_1\mathbf{T}_m\mathbf{F}_n, \quad m=28, \quad n=31. \tag{5} $$

Thus, climatic data, ${}_m\mathbf{F}_n$, are transformed into estimates of ring-width indices, ${}_1\hat{\mathbf{P}}_n$, via a transfer or response function, ${}_1\mathbf{R}_p\mathbf{E}_m$, denoted by the column vector, ${}_1\mathbf{T}_m$. The same eigenvectors and amplitudes may be used to derive transfer functions for several chronologies in a given region, because only the regression coefficients vary. The matrix manipulations described above involving eigenvectors have the advantage that the amplitudes, ${}_p\mathbf{X}_n$, are unlike the original data, ${}_m\mathbf{F}_n$, in that they are orthogonal or uncorrelated. This orthogonality allows the efficient use of stepwise multiple regression techniques to obtain ${}_1\mathbf{R}_p$ and then ${}_1\mathbf{T}_m$.

The ring-width index for a particular year is not independent of prior growth. This effect can be assessed by including in analyses the values of the three prior ring-width indices, thus obtaining the first, second and third-order autocorrelations (${}_1\mathbf{R}_3{}^*$). The estimation of ${}_1\mathbf{P}_n$ made with this enlarged set of predictors is accomplished by adding ${}_1\mathbf{R}_3{}^*\mathbf{Z}_n$ to the original estimates, ${}_1\hat{\mathbf{P}}_n$, where ${}_3\mathbf{Z}_n$ is a matrix of the growth indices for the three years prior to each yearly value of ring index entered in the column vector ${}_1\mathbf{P}_n$.

When estimating ${}_1\mathbf{P}_n$ using the transfer or response function, ${}_1\mathbf{T}_m$, the variance accounted for is a direct measure of the amount of information about the climatic variables contained in the chronology. The second estimation of ${}_1\mathbf{P}_n$ with the correction for prior growth accounts for more variance in ${}_1\mathbf{P}_n$ if autocorrelation in the ring-width chronology is important. The difference in the variance accounted for in the above two calculations (Table 1) provides a measure of the variance in the ring-width chronology attributed to autocorrelation and indicates a lag of one to three years in the response of ring growth to climate. A check was made on the residuals of ${}_1\hat{\mathbf{P}}_n$ from the actual data ${}_1\mathbf{P}_n$ to assure that the error was randomly distributed.

Confidence limits for each element of the transfer function, ${}_1\mathbf{T}_m$, can be found from their respective standard errors (see Draper and Smith, 1966, p. 19). In this study, these limits were obtained indirectly from the standard errors of the elements of ${}_1\mathbf{R}_p$ as defined in Eq. (4). The required transformation is

$$ {}_m\mathbf{S}_m = ({}_m\mathbf{E}_p\mathbf{U}_p\mathbf{U}_p\mathbf{E}_m')^{\frac{1}{2}}, \quad m=28, \; p=20, \tag{6} $$

where ${}_p\mathbf{U}_p$ is a diagonal matrix of the standard errors of the elements of ${}_1\mathbf{R}_p$, and ${}_m\mathbf{S}_m$ is a symmetric matrix the diagonal elements of which are the standard errors of the elements of ${}_1\mathbf{T}_m$. The 0.95 confidence limits are obtained by multiplying the right-hand side of (6) by the appropriate $\mathbf{F}$ value with v_1/v_2 degrees of freedom before taking the square root. Here v_1 is the number of significant (non-zero) elements of ${}_1\mathbf{R}_p$, and $v_2=n-2-v_1$.

At present the transfer (response) functions have been calculated for a sample of approximately 120 ring-width chronologies, many of which have been previously analyzed by other means (Fritts, 1965; Fritts *et al.*, 1965a; Julian and Fritts, 1968; Fritts, 1969a).

The median percent variance (or information) in the ring-width chronologies that is related to chronologies of the seasonal march of climate is approximately 60–65. This percentage is equivalent to the coefficient of determination or to linear correlations of 0.77–0.81. Only 20% of the ring-width chronologies have less than 50% variance related to the climate chronologies, while 20% of the ring-width chronologies have more than 80% variance related to climate.

Since many ring-width chronology sites were located near the margin or outside of the selected climatic regions, it is remarkable that more than half the variance in 80% of the ring-width chronologies is directly

TABLE 1. The percentage of variance in selected ring-width chronologies from Colorado that are related to chronologies of the seasonal march of climate and related to growth for prior years. The total explained variance, which is the sum of the first two columns, is also shown.

Sites	Species	Percent variance related to climate	Percent variance related to prior growth	Total percent explained variance
Owl Canyon	Pnn	62	30	92
Horsetooth Res.	PP	79	11	90
Waterdale	PP	67	25	92
Lyons	PP	82	15	97
Eldorado	PP	50	48	98
Van Bibber	PP	61	34	95
Kassler	PP	52	30	82
Horsetooth Sum.	DF	80	4	84
Big Thompson	DF	83	6	89
Eldorado Canyon	DF	85	0	85
Kassler	DF	80	1	81

Species: Pnn—*Pinus edulis*
PP—*Pinus ponderosa*
DF—*Pseudotsuga menziesii*

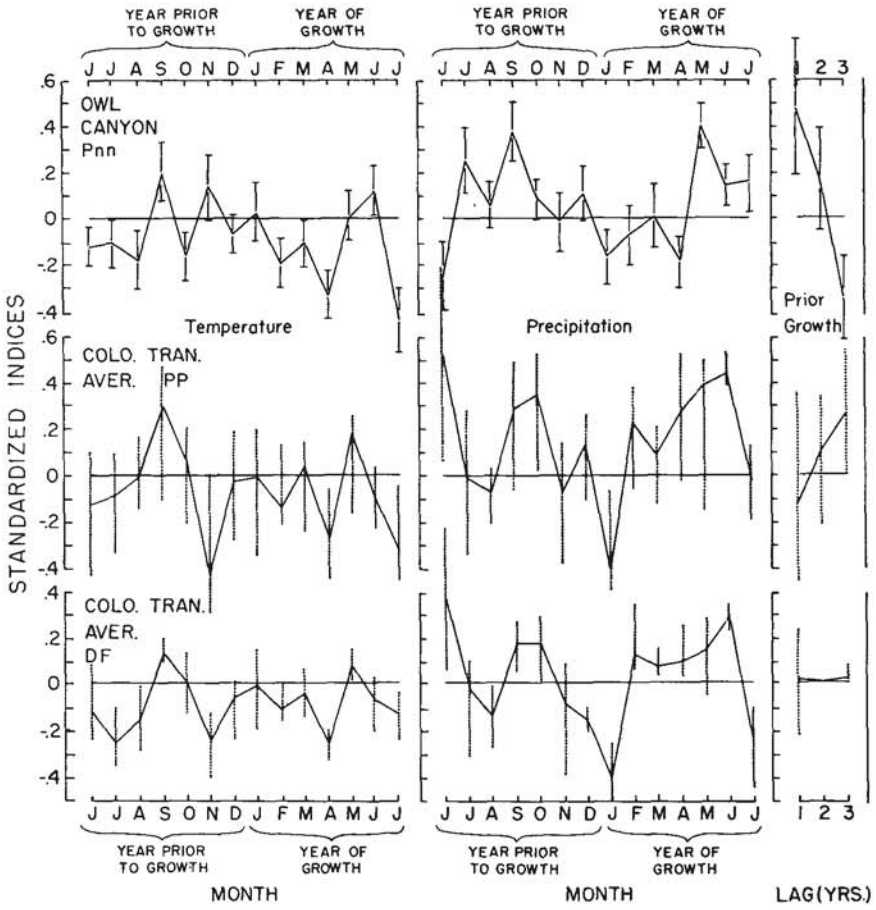

FIG. 4. The average response function, ${}_1T_{28}$, relating standardized ring-width indices for three species in Colorado to standardized average monthly temperature and standardized total monthly precipitation during the 14 months prior to and including the initiation of growth. Each point may be considered a weight associated with each climatic variable that will provide maximum reconstruction of the tree-ring chronology from the monthly climatic data. The plots may also be interpreted as the probable relative effect of a unit change in each climatic variable on a unit change in tree growth. The three variables on the right show the probable relationship with the width of the three prior rings. The dashed vertical lines show the maximum scatter of values obtained from separate analysis of individual sites. Ticks with solid vertical lines (shown for Owl Canyon) delineate the 0.95 confidence interval for each weight. (Pnn—*Pinus edulis*, *PP—Pinus ponderosa*, *DF—Pseudotsuga menziesii*.)

attributable to variations in the seasonal march of climate. The median variance attributed to autocorrelation within each ring-width chronology is 15% and the median total variance accounted for when including prior ring-width indices is 85–90%.

A survey of the plotted response functions, ${}_1T_m$, shows considerable detail, and the results are more interpretable in terms of the models shown in Figs. 1, 2 and 3 than similar results obtained in earlier studies using multiple regression to relate ring-width chronologies directly to climatic data (Fritts, 1962; Julian and Fritts, 1968). The response functions do vary among samples, but they are surprisingly consistent among different species within similar areas and sites. For example, the averages of the response functions for the six *Pinus ponderosa* (PP) sites and four *Pseudotsuga menziesii* (DF) sites included in Table 1 are shown in Fig. 4. The same chronologies were analyzed by Julian and Fritts (1968) using multiple regression with monthly temperature and precipitation values. The regression weights obtained through the multivariate approach appear more stable (i.e., do not vary as much between analyses of different sites) and are sometimes significantly different from the weights obtained by multiple regression (Julian and Fritts). These discrepancies apparently arise because multiple regression does a better job of handling interrelationships among the climatic variables when the original data are first subjected to principal component analysis.

The ring-width index for these two species is directly related to temperature in September and May and precipitation in the previous June, September, October, and February through June, while it is generally inversely related to temperatures during other months

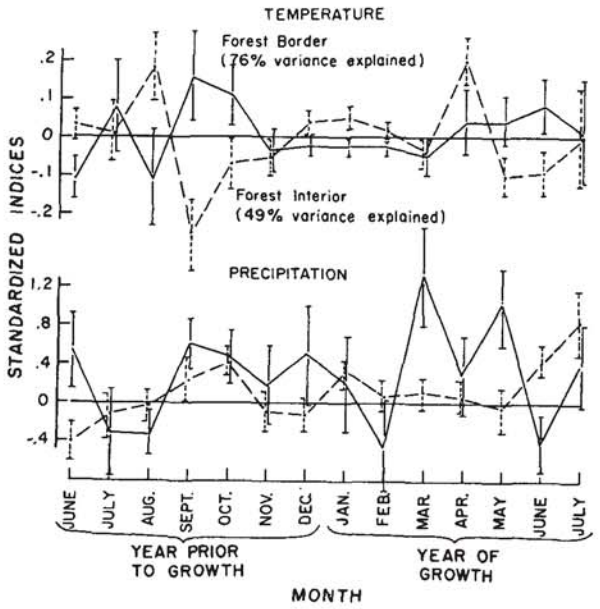

FIG. 5. The response function for ponderosa pine near the forest border (solid line) and in the forest interior (dotted line) of northern Arizona (Fritts, *et al.*, 1965b, sites C and B). Plots differ from those shown in Fig. 4 in that the weight for each climatic variable is divided by the standard deviation for that variable. In this form the plots may be interpreted as the relative effect of one degree Fahrenheit rise in mean temperature for the month and an inch increase of monthly precipitation on ring-width growth expressed in standard normal form. The ticks with vertical lines delineate the 0.95 confidence interval.

of the year and to precipitation in late summer of the prior year and during early or mid-winter. However, the growth of PP is more related to prior growth than DF (Table 1), and the response functions vary more from site to site (Fig. 4). The response function for a stand of *Pinus edulis* (Pnn) in the same area is also shown. This species is at its northern limit on this site and exhibits some differences in response from those of the other two species, but the chronology contains almost as much information on climate (Table 1). Temperatures in September, November and the following June are directly correlated with its growth. High temperatures at the beginning or end of the growing season may extend its length, which favors the formation of a wide ring. At other times, except for November, temperatures are inversely correlated with growth as they may enhance water loss and respiration which consume available moisture and stored foods. Precipitation is directly related to growth except late in the prior summer and during mid-winter when heavy snow cover, reduction of light intensities due to cloud cover and low temperatures may adversely influence the trees and affect the next year's growth (see Figs. 1, 2 and 3). Other plots of response functions show systematic changes from low to high latitude sites and from low to high elevations.

A somewhat different representation of the response functions is shown in Fig. 5. Each element of the response or transfer function, ${}_1\mathbf{T}_m$, and their 0.95 confidence limits are divided by the standard deviation of the corresponding set of climatic data. This converts the elements to relative measures of the effect of a one degree Fahrenheit rise in temperature and an inch increase in precipitation for separate months of the year upon ring-width growth (effects of temperature and precipitation decreases are obtained by reversing the signs). Response functions of this form as shown for two groups of PP, one being a stand near the arid lower forest border (solid line, stand C) and the other a stand in the forest interior near Fort Valley, Ariz., (dashed line, stand B), both from Fritts *et al.* (1965b). A total of 76% of the ring-width variance of the forest border stand is related to climate as the trees were highly limited by environmental variables. Only 49% of the variance of the ring-width chronology from the forest interior stand is related to climate. These forest interior trees have also been intensively investigated by Glock and others (1964, 1969).

Fig. 5 shows marked differences between the growth responses of trees along the forest border and trees in the forest interior. The responses to temperature on the two sites are diametrically opposite in sign. The response to precipitation on the arid site is marked and direct for ten months in the year and inverse only for the previous July, August and February and the current June. The response for forest interior trees to precipitation is most marked in June and July. Apparently the growth of trees on the forest border site is more influenced than growth on the interior site by precipitation falling at times other than the growing season. The differences shown in these plots explain how forest interior trees like those reported by Glock and Agerter (1969) differ in their response to climate from trees on the more limiting, warm and arid sites reported by Fritts (1965). They also show the wide diversity in response obtainable from trees on neighboring but ecologically contrasting sites.

4. Reconstructing anomalies in past climate

a. Development of model

It is well accepted that variations in the width of the annual rings of trees on a given site may reflect a significant amount of information about fluctuations of the local environment. However, these fluctuations also may be manifestations of large-scale regional anomalies. These regional anomalies will be systematically reflected in spatial anomaly patterns of ring widths from groups of trees representing sampled sites. Such regional patterns in tree-ring widths have been identified via principal component analysis (LaMarche and Fritts, 1971). The results indicate that a large percentage of tree-ring variance is incorporated into regional anomaly patterns which cannot be a reflection of purely local factors but may be closely related to large-scale anomalies in the general atmospheric circu-

lation (Sellers, 1968). These anomalies may occur in the year prior to, as well as in the year during which growth takes place. It is the purpose of this section to identify some seasonal climatic anomaly patterns which can be specified from given tree-ring data, to quantify our estimating procedure using recorded climatic data for calibration, and to extend the resulting statistical relationships to estimate patterns of circulation anomaly during periods for which tree-ring data are available but climatic data are not.

Previously selected replicated tree-ring chronologies at 49 locations in western North America were used for this analysis. The first four eigenvector patterns of tree growth (eigenvectors of the correlation matrix formed from the 49 chronologies) are presented by LaMarche and Fritts (1971). The first seven eigenvectors describe large-scale regional patterns and explain 57% of the total tree-ring variance for the period 1700–1930 A.D. This result suggests that over half of the tree-growth variance is related to large-scale macroclimatic anomalies and that spatial patterns of tree-growth chronologies may be used to reconstruct the patterns of atmospheric circulation that produce the macroclimatic anomalies.

As noted above, the present analysis is concerned with the estimation of seasonal rather than monthly circulation patterns. A seasonal climatic anomaly pattern is taken to be the pressure anomaly field for a three-month period. The months comprising each season were selected so as to correspond as closely as possible to the "natural" seasons and subseasons as presented by Bryson and Lahey (1958).

The spring season (which includes approximately the first half of the growing season) and the preceding winter season correspond to the year of ring growth, while autumn and summer refer to the previous year. The seasons are identified as follows:

Summer: July, August, September
Autumn: October, November, December
Winter: January, February, March
Spring: April, May, June

Normalized values of the seasonal sea-level pressure were used as climatic data. They were computed from monthly values provided by the Extended Forecast Branch of the U. S. Weather Bureau. The analysis grid consisted of 100 points located primarily over the western half of the Northern Hemisphere; points were located every 10° of latitude and longitude from 25 to 65N and from 165E to 5W.

The first 8 eigenvectors of the pressure anomaly field for each season were computed. The resulting 32 eigenvectors of pressure fields and the 7 eigenvectors of tree growth fields comprise 2 sets of variables. The amplitudes, or multipliers, of these variables (${}_p\mathbf{X}_n$) were obtained as in Eq. (3), where ${}_m\mathbf{E}_p$ and ${}_m\mathbf{F}_n$ refer to the eigenvector and data matrices defined above. The subscripts of these matrices are as follows: for the eigenvectors of pressure fields, $p=8$ for each season, $m=100$ grid points, and $n=62$ years of data (1899–1966, excluding 1939–44); for the eigenvectors of tree growth fields, $p=7$, $m=49$ sites, and $n=231$ years of data (1700–1930). By including independent tree-ring data from the years (1931–62) in ${}_m\mathbf{F}_n$ of Eq. (3), amplitudes were also obtained for these recent years. Thus, in the complete ${}_p\mathbf{X}_n$ matrix, $n=231+32=263$ years (1700–1962).

For the 57 years (1900–62, excluding 1939–44) common to both data sets, the corresponding amplitude chronologies were subjected to a canonical correlation analysis as presented by Glahn (1968). The components of the resulting canonical variates weight the amplitudes of the tree-growth field eigenvectors in such a way that they are canonically correlated with weighted amplitudes of the pressure-anomaly field eigenvectors. Since the eigenvectors of pressure patterns *for all* seasons were included, the weighted assemblages of the eigenvectors of tree-growth patterns are related to weighted assemblages of the eigenvectors of pressure patterns for all seasons. Then, following the canonical regression model described by Glahn, it is possible to estimate normalized pressure anomaly fields from canonically weighted eigenvectors of tree-growth fields using tree-growth data from periods prior to the beginning of climatic records. At the time this research was carried out, a different regression scheme (described below) was used. Subsequent computations have shown that both methods produce almost identical results.

In the work reported here, estimates of the normalized pressure anomalies at each grid point were made using multiple regression functions of the canonically weighted amplitudes of the tree-growth field eigenvectors. The equations are identical to those used in the previous section except for the introduction of the additional canonical weighting functions. The estimation model was developed as follows, using the 57 years of concurrent data:

$$ {}_1\hat{\mathbf{P}}_n = {}_1\mathbf{R}_p\mathbf{X}_n^*, \quad n=57,\ p=7, \tag{7} $$

where ${}_1\hat{\mathbf{P}}_n$ denotes n estimates of the pressure anomaly for a particular grid point and season, ${}_1\mathbf{R}_p$ is the row vector of multiple regression parameters, and ${}_p\mathbf{X}_n^*$ is the matrix of canonically weighted amplitudes of p tree-growth field eigenvectors for n years (${}_p\mathbf{X}_n$). That is,

$$ {}_p\mathbf{X}_n^* = {}_p\mathbf{W}_p\mathbf{X}_n, \quad n=57,\ p=7, \tag{8} $$

where ${}_p\mathbf{W}_p$ is the complete matrix of canonical variates corresponding to tree-growth variables. Thus, substituting (8) into (7), and using the relation given in (3), we have

$$ {}_1\hat{\mathbf{P}}_n = {}_1\mathbf{T}_m\mathbf{F}_n, \quad m=49,\ n=57, \tag{9} $$

where the transfer function, ${}_1\mathbf{T}_m$, is given by

$$ {}_1\mathbf{T}_m = {}_1\mathbf{R}_p\mathbf{W}_p\mathbf{E}_m', \quad m=49,\ p=7. \tag{10} $$

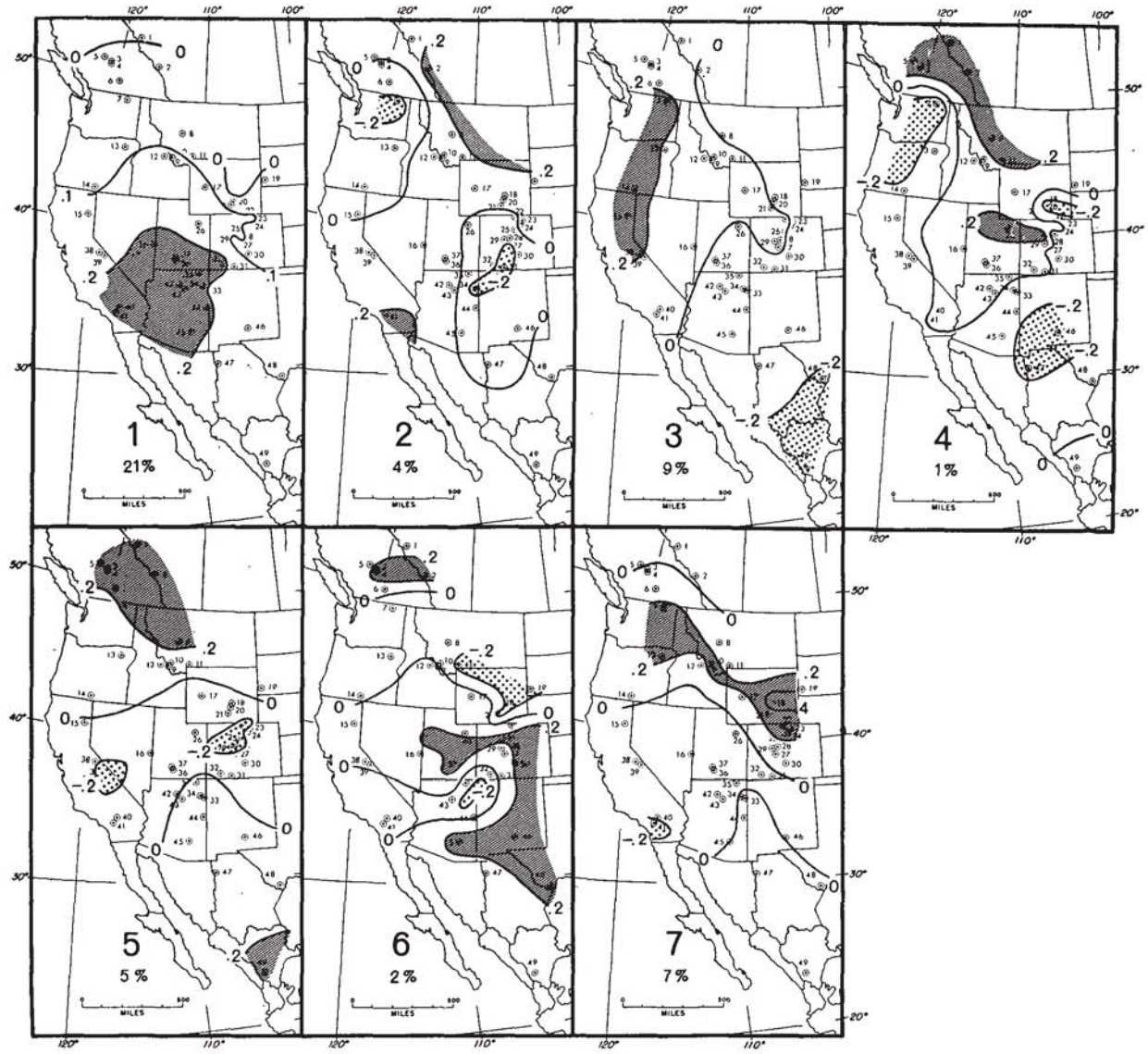

FIG. 6. Plots of the seven eigenvectors of anomalous tree growth, ${}_7\mathbf{W}_7\mathbf{E}_{49}'$, weighted to give maximum correlation with surface pressure anomalies. Plots are ranked from high to low correlation with pressure anomalies, and the percentage represents the variance in tree growth explained by each eigenvector. Dots on maps locate the 49 tree-ring collection sites.

This transfer function transforms a matrix of normalized tree-ring data into estimates of seasonal pressure anomaly at an individual grid point. Thus, (9) is identical in form to (5). The canonical weight matrix, ${}_p\mathbf{W}_p$, is used to weight the amplitudes of the tree-growth field eigenvectors such that their correlation with spatial patterns of pressure anomaly for all seasons is maximized. As shown in Eqs. (8) and (10), the matrix, ${}_p\mathbf{W}_p$, can be applied to either the amplitude matrix, ${}_p\mathbf{X}_n$, or the eigenvector matrix, ${}_m\mathbf{E}_p$.

The first 7 weighted eigenvectors of tree-growth patterns, ${}_7\mathbf{W}_7\mathbf{E}_{49}$, are shown in Fig. 6 and the corresponding weighted amplitudes, ${}_7\mathbf{X}_{263}{}^*$, for the period 1700–1962 are shown in Fig. 7.

Maps of the regression weights, ${}_1\mathbf{R}_1$, which relate the canonically-weighted amplitudes of the tree-growth field eigenvectors to pressure estimates at each of the 100 grid points are presented, for each season, as Figs. 8, 9 and 10. The values of the regression weights are contoured and the three figures may be interpreted as representing the anomalous pressure patterns giving rise to the climatic patterns associated with the first three eigenvector patterns of tree growth illustrated in Fig. 6. Brief descriptions of possible relationships between the anomalous pressure patterns and the climatic patterns associated with anomalous tree growth are included in the figure captions. Finally, from Eq. (7) it can be seen that the mapped regression weights,

when multiplied by the weighted amplitudes of the tree-growth field eigenvectors, shown as Fig. 7, can provide estimates of the pressure anomaly patterns.

Spatial patterns of the percentage of pressure variance explained using the estimation model [Eq. (7)] over the period of the dependent data (1900–39, 1945–62) are shown in Fig. 11. These patterns indicate where the best estimation of pressure was obtained. The percent of normalized pressure variance for each season accounted for by the equations was: summer, 23.7%; autumn, 20.6%; winter, 24.0%; and spring, 18.5%. These spatially averaged percentages are somewhat unrepresentative as the actual patterns of explained variance generally indicate better prediction over or "upstream" of the sites of tree growth and areas of poorer prediction "downstream" of the tree sites (see Fig. 11). Thus, higher percentages of variance would have been obtained if the pressure grid had been chosen differently.

It should be mentioned that the average figure of about 20% of pressure variance explained in each season is more significant than might appear, for the ring-width variability of the trees used in this analysis is primarily an integrated measure of the limiting effect of low moisture and high temperatures throughout *all seasons* of the year (Figs. 1 and 2). Thus, assuming the possibility of a perfect response of these particular trees to climate at all pressure grid points and all four seasons, but assuming that no linear correlation between the pressure patterns of the four seasons, one would expect an average of 25% of variance explained in each season rather than 100%. It would therefore appear that an average of 20% for each season is an encouraging result, especially considering the choice of grid, as described above. As new species, and trees with more diverse response functions are added to the original tree-ring data set, and the areal coverage of the pressure grid is reduced or limited to the region over and "upstream" of the tree sites, it should be possible to improve prediction of the anomalies in climate for the separate seasons.

b. Application of model

Using Eq. (7) ($n=57, p=7$), the tree-ring data in the form of weighted eigenvector amplitudes shown in Fig. 7 for each year, 1700–1899, were used to estimate past anomalies in pressure at each of the 100 grid points of the half-hemisphere grid for each of the four seasons. [Eq. (9) could also have been used, which utilized directly the tree-ring data at the 49 sites, and the weighted eigenvectors show in Fig. 6 instead of using the amplitudes.] The 200 estimated, normalized pressure anomalies for each grid point and season, $_1\mathbf{P}_{200}$, were then converted to millibar pressure anomalies by multiplying each normalized pressure estimate by the standard deviation of pressure for the corresponding grid point and season. These standard deviations were

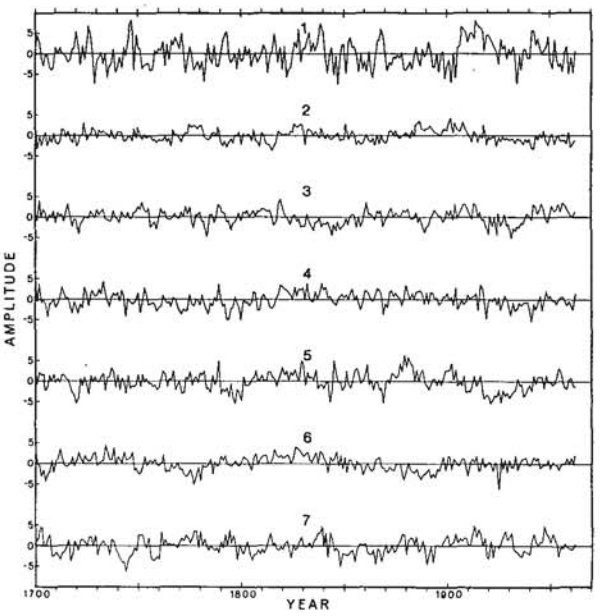

FIG. 7. Plots of the amplitudes for the seven eigenvectors of anomalous tree growth, $_7\mathbf{X}_{263}$*, weighted to give maximum correlation with surface pressure anomalies. Plots are ranked from high to low correlation with pressure anomalies.

obtained from the dependent period. Estimates of mean pressure for each season and year of the period 1700–1899 were obtained by adding to the millibar anomaly the mean pressure (the mean for the dependent period) for each point and season.

The estimated mean and anomalous grid point pressure values for each season, averaged by pentads and by decades, were plotted and contoured by computer. Selected pressure anomaly maps (in millibars) for winter are shown in Figs. 12, 13 and 14. The square dots indicate that the five-year mean departures are greater than twice the standard error.

A preliminary attempt has been made to provide some measure of verification of the reconstructed pressure maps using published decadal maps of January pressure which cover the North Atlantic sector (Lamb and Johnson, 1966). Unfortunately, the reliability of the reconstructed maps is expected to be poor over the North Atlantic as the explained dependent variance is particularly low in this sector (Fig. 11). In addition, the published maps are for monthly means while the reconstructed maps are for the entire season. Thus, the preliminary verification presented below cannot be considered a final test of the model.

Three broad comparisons of the North Atlantic sector of the reconstructed winter maps with the observed January maps for the 19th century are summarized in 3×3 contingency diagrams in Table 2. In general, the decadal pressure maps reconstructed from tree-ring data do provide information about the position of the Icelandic low (Table 2a); however, it was found that specifications of its intensity were not accurate. The

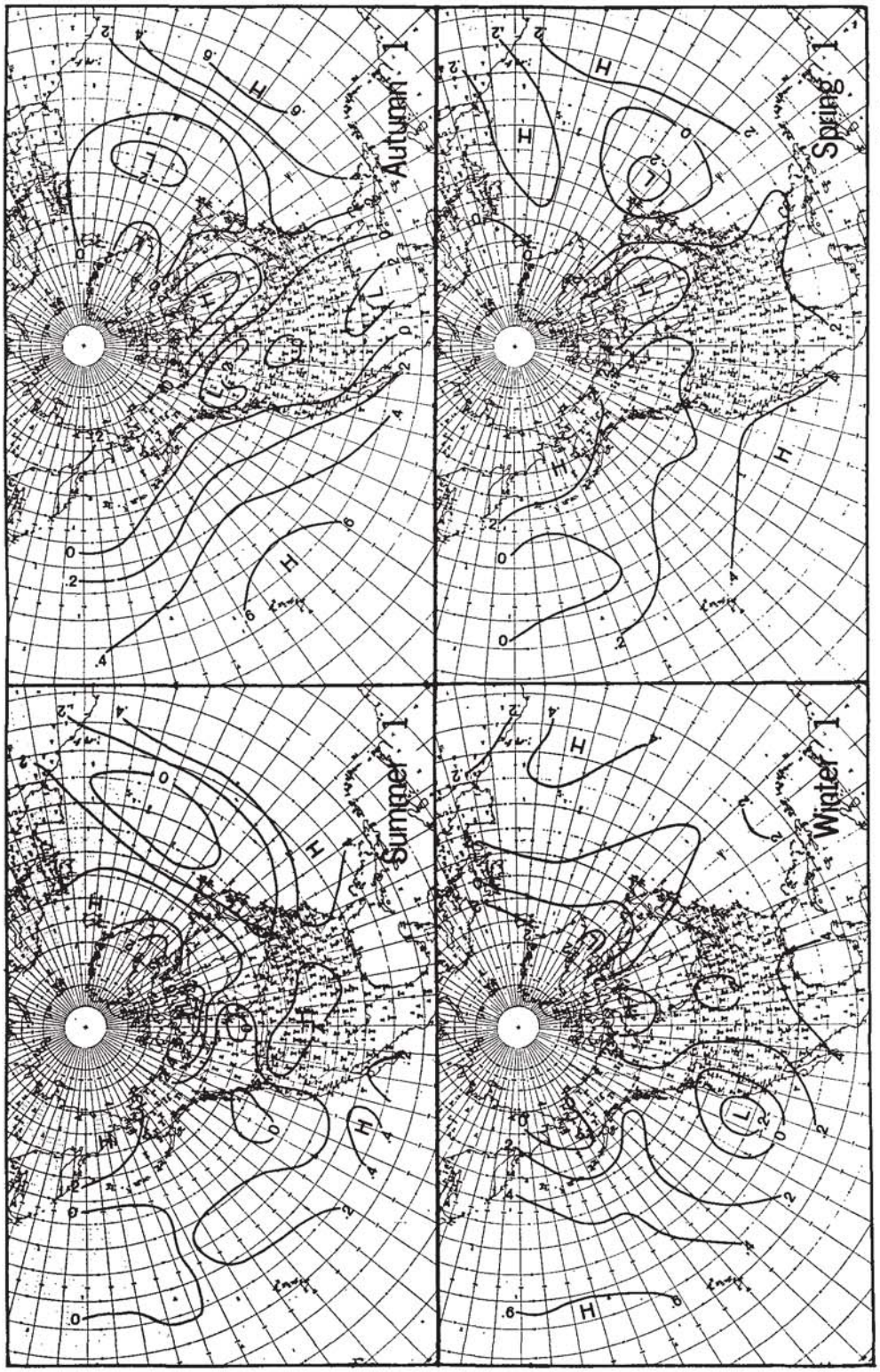

FIG. 8. Maps of the regression weights, $\mathbf{R}_1$, relating tree growth variable 1 to pressure anomalies in each of the four seasons. Each regression weight is plotted at the corresponding station location so that contours show the anomalous circulation patterns that are associated with patterns of anomalous growth shown in Figs. 6 and 7. High growth in Arizona and southern California results from increased flow of moisture into the region associated with increased southern flow over southwestern North America in summer and winter. Associated features indicated by the maps include: 1) In summer, an apparent subtropical high pressure system extends across the United States, and zonal flow is decreased at high latitudes over the North Atlantic. 2) In autumn, there are two regions of increased cyclonic activity over Alberta and Texas. The flow is more zonal at low latitudes over the North Atlantic. Increased ridging is observed over the north pole. 3) In winter, a region of low pressure anomaly persists off the California coast, and the Icelandic low is displaced westward and intensified. Subtropical highs are also intensified. 4) In spring, higher than normal pressure dominates North America, particularly over Hudson's Bay, and a low pressure anomaly is conspicuous off the Newfoundland coast, increasing meridianal flow off the east coast of North America.

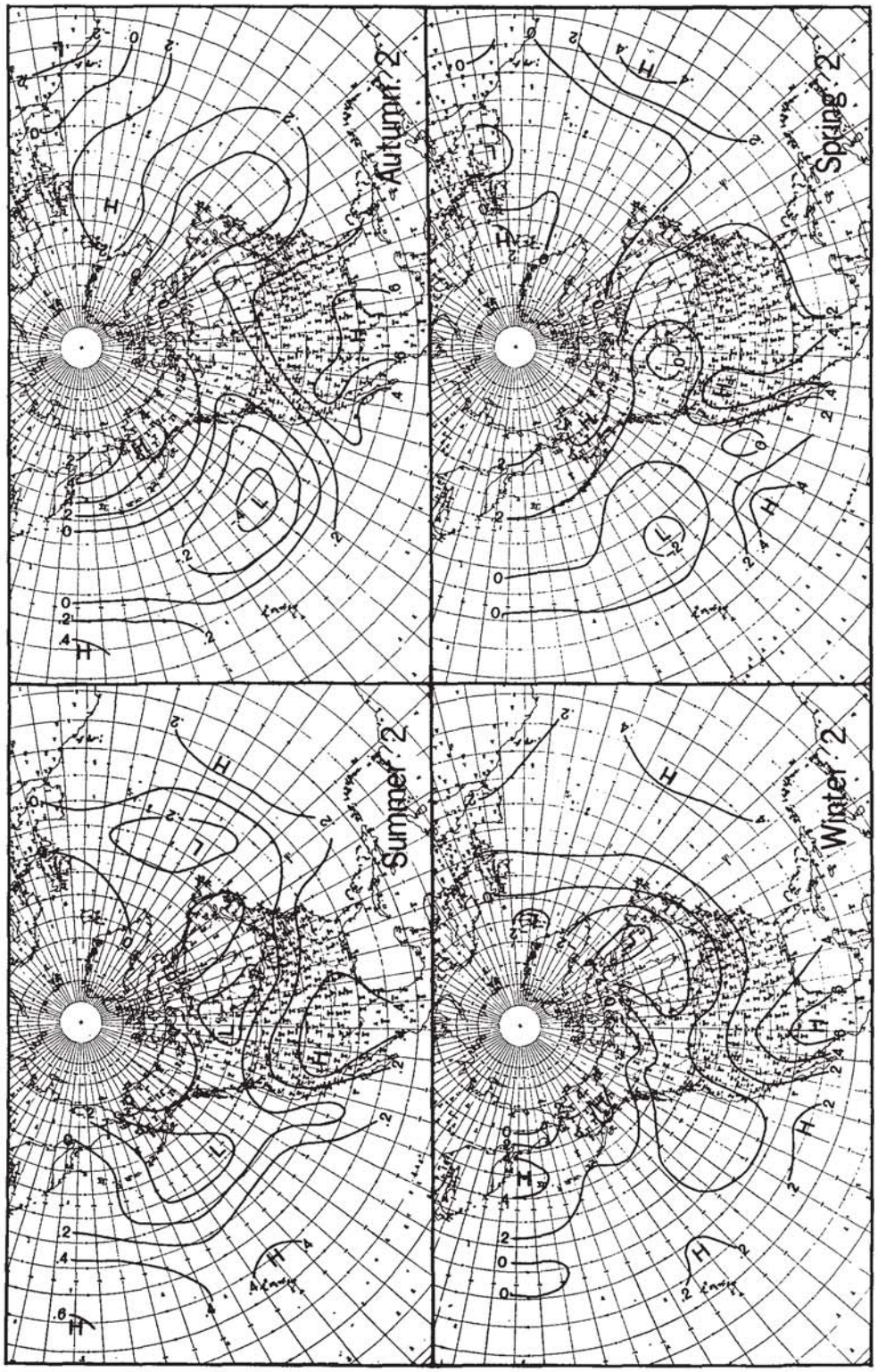

FIG. 9. Maps of the regression weights, $_1R_1$, relating tree-growth variable 2 (Figs. 6 and 7) to pressure anomalies in each of the four seasons (see legend to Fig. 8). High growth centering in the regions on the east slope of the Northern Rockies and in southern California is associated with low growth in the southern Rocky Mountains and in the Pacific Northwest. This pattern is associated with positive pressure anomalies in all seasons over the southwestern deserts and in the Great Basin; thus, the flow from the Gulf of Mexico into the southern Rocky Mountains is reduced. The low growth in the Pacific Northwest results from an apparent deflection of storm tracks to the north of that area especially in spring and summer. Associated features indicated are: 1) In summer, the subtropical highs are weakened or displaced southward over the oceans. 2) In autumn, the Aleutian low is expanded and/or displaced southward; pressures are anomalously high over North America except for the Northeast Coast, and there is an increased tendency for blocking over the North Atlantic. 3) In winter, the Icelandic low appears expanded, intensified, and perhaps displaced to the southwest. 4) In spring, the Aleutian low is displaced southward.

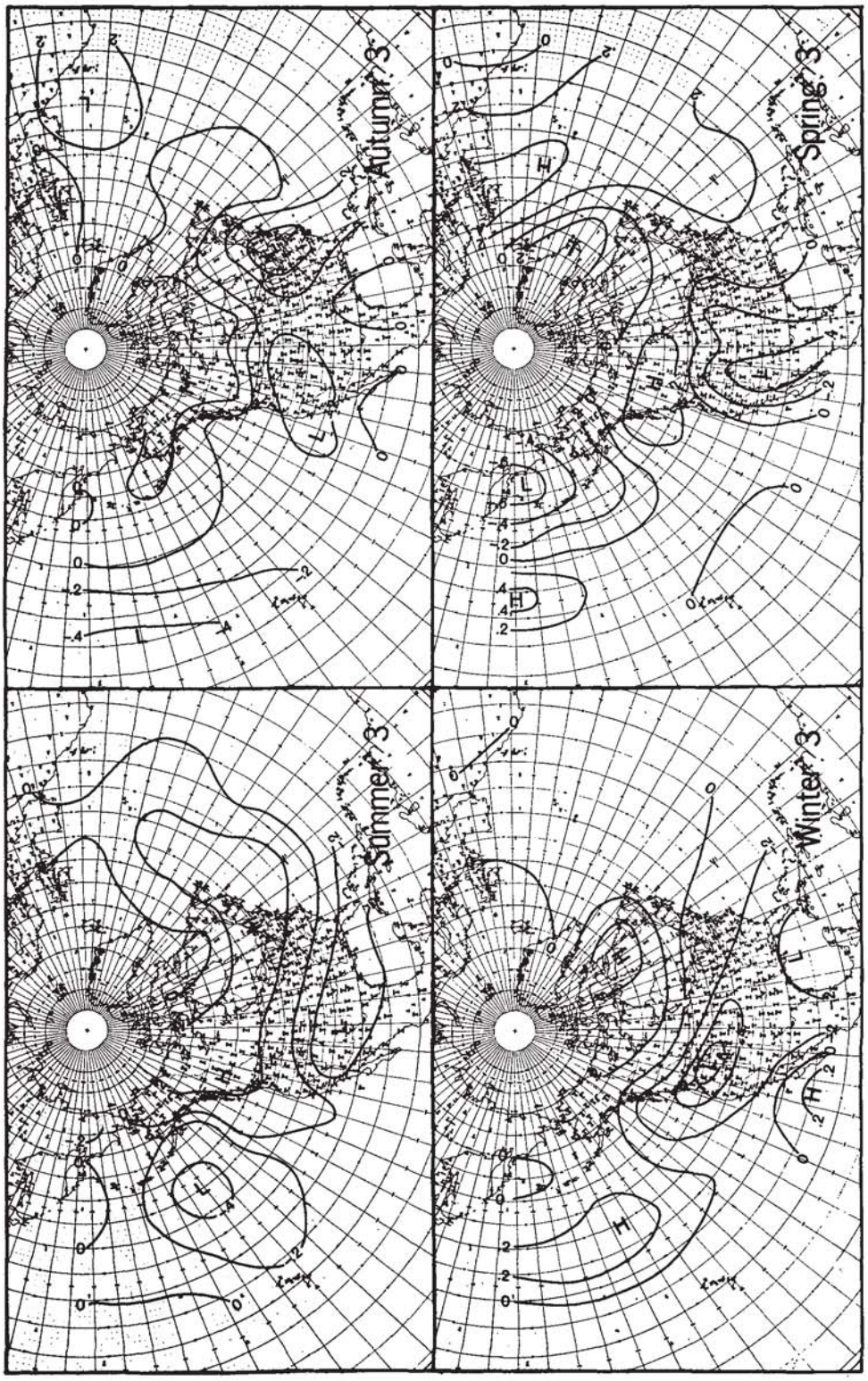

FIG. 10. Maps of the regression weights, ${}_1R_1$, relating tree growth variable 3 (Figs. 6 and 7) to pressure anomalies in each of the four seasons (see legend to Fig. 8). High growth in Washington, Oregon and northern California along with low growth in west Texas and western Mexico is associated with favorable temperature and moisture (without extremely cold weather) over the Northwest and dry conditions in the Southwest. These conditions result from a generally weakened zonal flow over North America in all four seasons. Associated features indicated by the map are: 1) In summer, the Pacific high is weak and the Bermuda high does not extend westward so little moist air flows into the Southwest. 2) In autumn, there is increased cyclonic activity over the Great Basin and eastern North America. The Pacific high is weak and zonal flow is reduced over the central Pacific. 3) In winter, anomalous cyclonic activity is primarily restricted to the Pacific Northwest. 4) In spring, both the Aleutian and Icelandic lows are displaced westward and a low is well developed over Arizona, bringing dry warm air from Mexico.

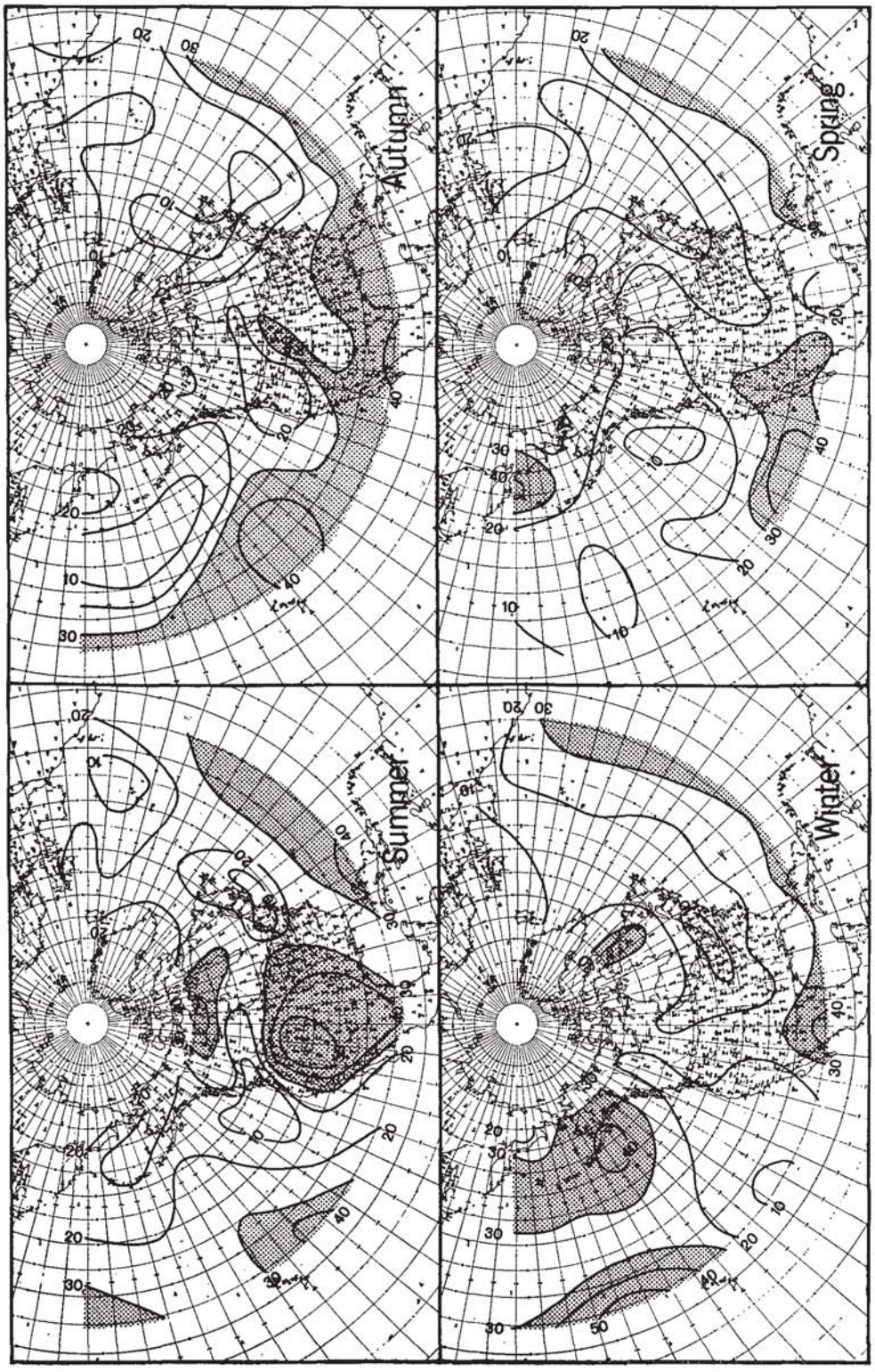

FIG. 11. The percentage variance in surface pressure anomalies explained by the tree-ring data for the period 1900–39, 1945–62. The shaded areas represent areas where the explained variance is most significant (>30%). During all four seasons prediction is high over the subtropical oceans. Prediction is greatest during summer over western North America and north-central Canada, during autumn over the high plains, during winter over the Aleutian Islands and Coast of Labrador, and during spring over the Bering Sea.

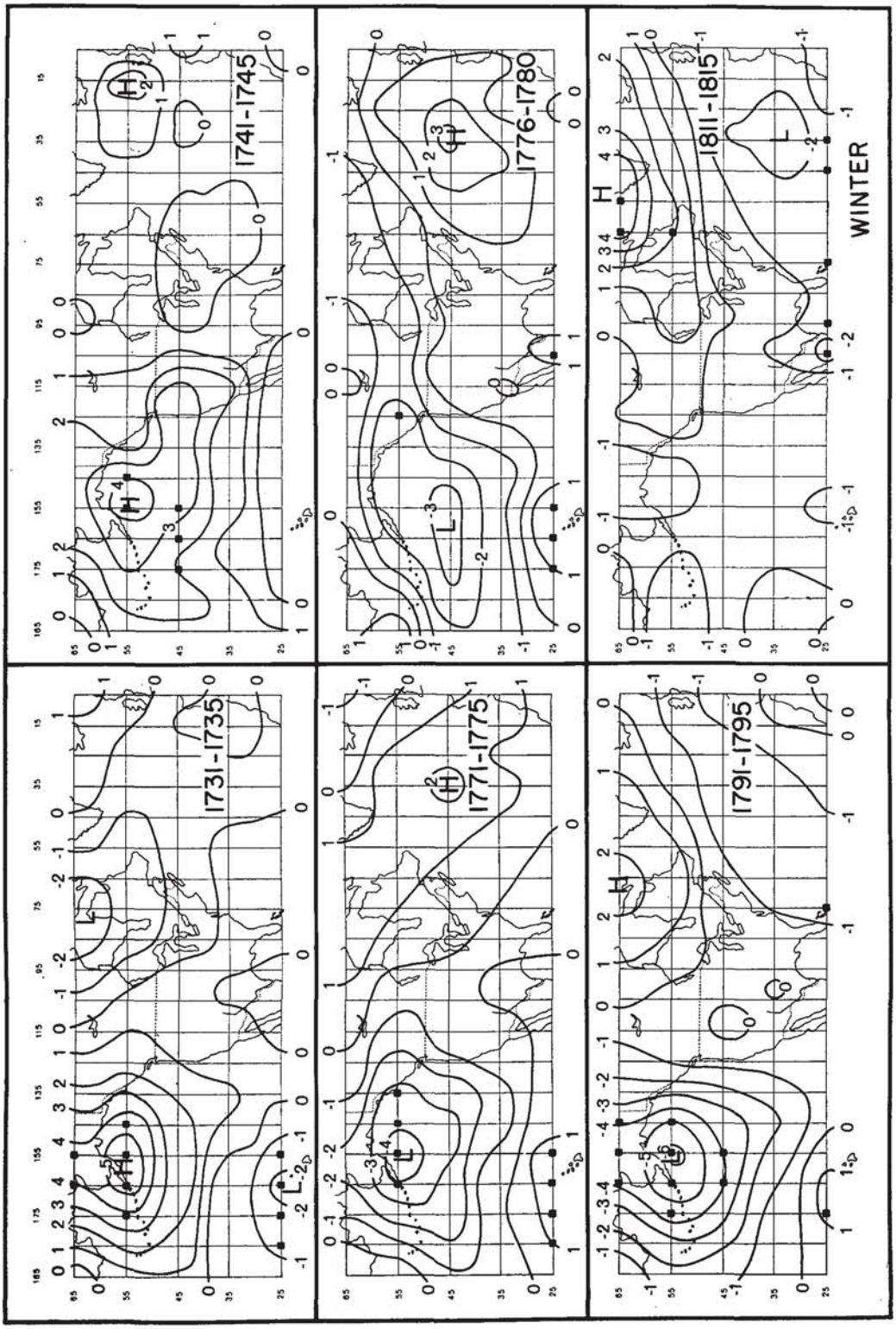

FIG. 12. January through March pressure anomalies for selected pentads of the period, 1700–1815, expressed in millibars and averaged by pentads, as specified from anomalies in tree growth. A square dot indicates that the five-year mean anomaly at the grid point was greater than twice the standard error, $\sigma/\sqrt{5}$, where σ is the standard deviation of the residuals, ${}_1P_{57}-{}_1\hat{P}_{57}$. Only maps with five or more departures exceeding two standard errors are shown.

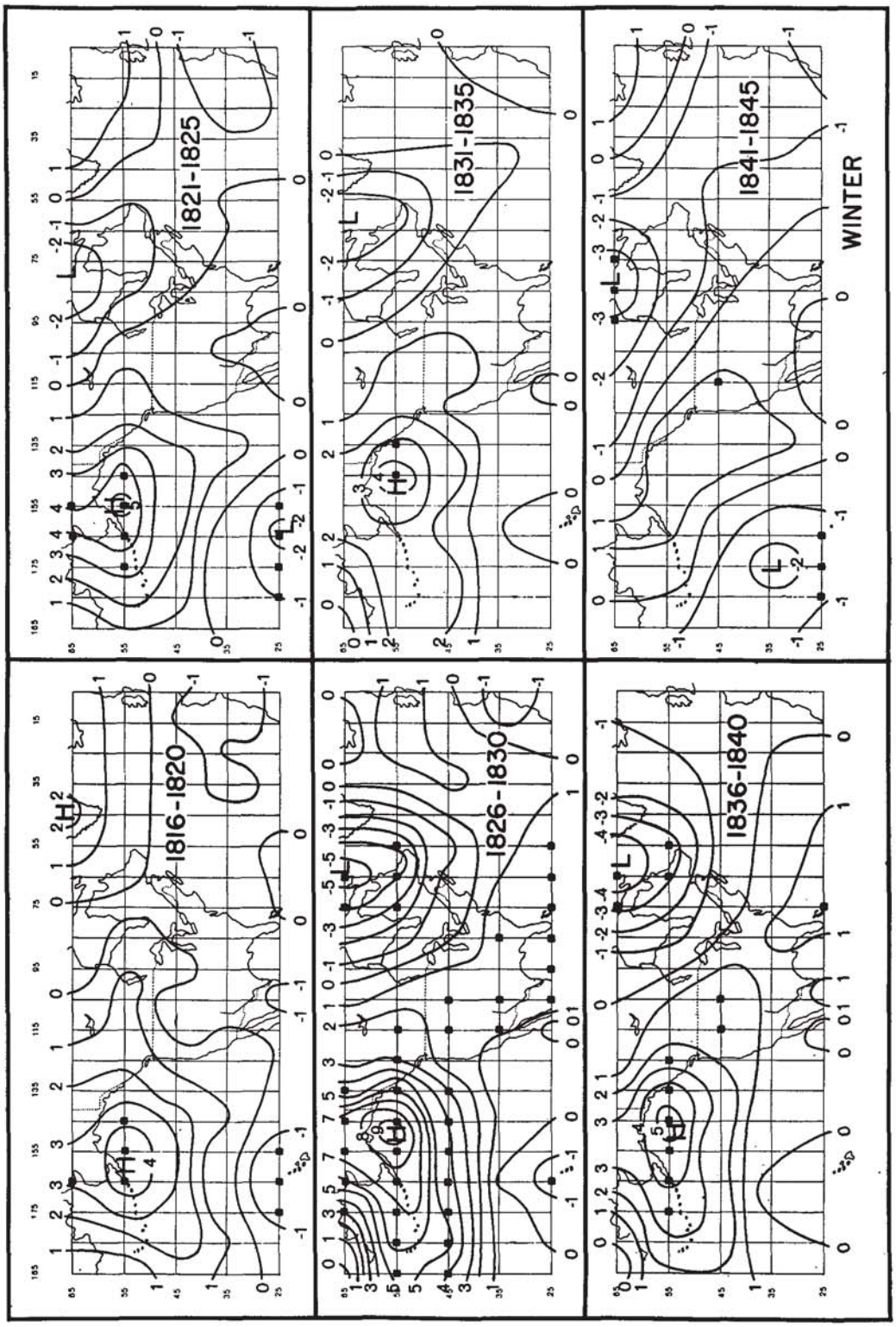

FIG. 13. January through March pressure anomalies from 1816–1845 expressed in millibars and averaged by pentads as specified from anomalies in tree growth. A square dot indicates that the five-year mean anomaly at the grid point was greater than twice the standard error, $\sigma/\sqrt{5}$, where σ is the standard deviation of the residuals, ${}_1P_{57}-\hat{P}_{57}$.

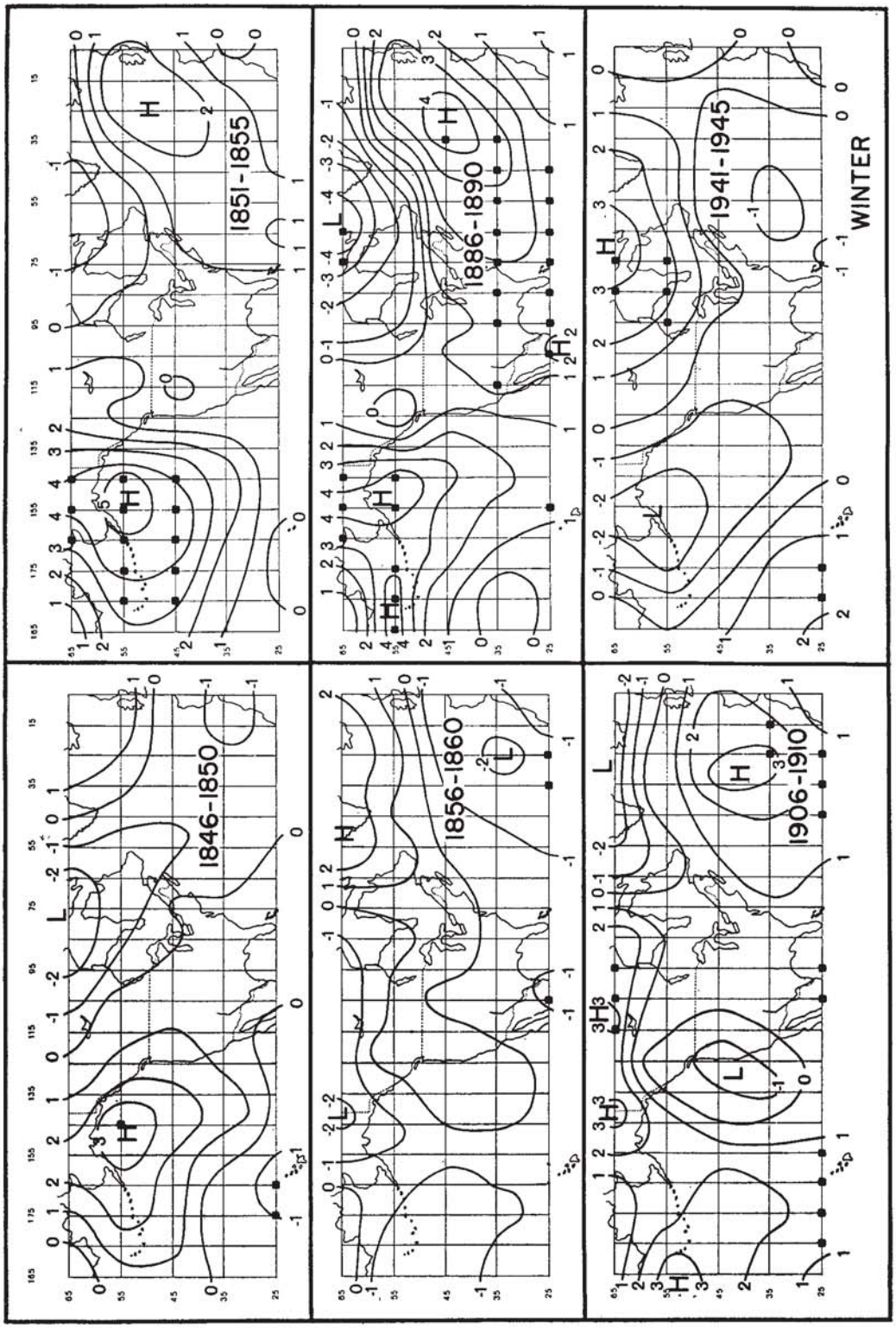

FIG. 14. January through March pressure anomalies for selected pentads of the period 1846–1960 expressed in millibars and averaged by pentads as specified from anomalies in tree growth. A square dot indicates that the five-year mean anomaly at the grid point was greater than twice the standard error, $\sigma/\sqrt{5}$, where σ is the standard deviation of the residuals, ${}_1P_{87}-{}_1\hat{P}_{57}$. After 1860 only maps with five or more departures exceeding two standard errors are shown.

pressure pattern anomalies predicted from tree rings also provide some information on the intensity (Tables 2b and 2c) and approximate location of the North Atlantic subtropical anticyclone, although detailed specification of its position was not obtained. An apparent reduction in the prediction of pressure anomalies lasting several decades or longer was also noted. This reduction of prediction is to be expected because the density of forest stands on semiarid sites may change slowly in response to persistent anomalies in climate. Such changes reduce the amount of low-frequency variance that can be retained in the ring-width record (Fritts, 1969b) so that it becomes a source of information emphasizing relatively short-term climatic changes.

While the verification results in the Atlantic sector do not indicate strong quantitative association, there is an apparent qualitative association between Lamb's maps and those derived from tree-ring information. Thus, considering that the verification scheme compared a season (winter) with a month (January) and considering that the explained variance for the dependent sample was lowest in the North Atlantic sector, there is reason to expect more reliable paleoclimatic reconstruction in areas of higher explained variance over North America and the North Pacific (Fig. 11), especially in regions that coincide with prominent features of the general circulation, such as the Aleutian low and the Pacific subtropical high.

TABLE 2. A comparison for the North Atlantic sector of decade maps of pressure during the 19th century derived from tree-ring data with the historical data published by Lamb and Johnson (1966).

a. Longitude of lowest pressure of the Icelandic low along 65N

		January maps (observed)*		
		West of Greenland	Near Greenland	East of Greenland
Winter maps (reconstructed from tree-ring data)	West of Greenland	2	0	0
	Near Greenland	0	2	0
	East of Greenland	0	1	4

b. Pressure of the subtropical anticyclone near the east coast of North America

		January maps (observed)		
		Below normal	Near normal	Above normal
Winter maps (reconstructed from tree-ring data)	Below normal	2	0	0
	Near normal	0	2	3
	Above normal	2	0	1

c. Pressure of the subtropical anticyclone near the west coast of Africa

		January maps (observed)		
		Below normal	Near normal	Above normal
Winter maps (reconstructed from tree-ring data)	Below normal	2	2	0
	Near normal	1	0	2
	Above normal	0	1	2

* Decade 1800–09 not classified.

5. Discussion and conclusions

In the first portion of this study, principal component (eigenvector) analysis was used to transform tree-ring or climatic data to a reduced number of orthogonal variables. Selection of the most important of these orthogonal variables enables one to retain the large-scale regional components which may represent the macroclimatic "signal" and to eliminate the more random components or "noise." Furthermore, it was efficient to use the orthogonal variables in stepwise multiple regression analyses. Transfer or response functions were obtained by combining multivariate and multiple regression techniques. These transfer functions allowed the measurement of rather subtle differences in the growth responses among trees on different sites.

The results from such use of multivariate analyses do not prove causation. However, they can be interpreted in terms of cause and effect if they are reasonable and consistent with expected physiological models and with current knowledge of the energy and water budgets of the respective trees and sites. For example, when temperature and precipitation for any given month are highly correlated, they will be included in some of the same eigenvectors and are both likely to appear in the response function. Many of the response functions from arid-site trees show that high temperatures and low precipitation are jointly associated with low growth. It could be argued that only one of these variables actually limited growth, but because of the intercorrelation, it would be impossible in the above type of analysis to distinguish which is a causal and which is a correlated effect. However, it can be shown that temperature and precipitation are not only highly correlated, but that they interact by jointly affecting water relations and physiological processes that become limiting to growth of trees on semi-arid sites. Since these two factors can be shown to act in consort, they should both be considered as a part of a factor complex which limits growth.

In other cases, such as in analysis of trees from well-drained sites at the upper timberline, there is good evidence that low temperature rather than high moisture may become limiting to growth. In such cases, when both variables are entered in the response functions in an inverse manner, it would be most appropriate to interpret the apparent inverse relationship between growth and precipitation as a correlated rather than a causal effect.

In the second portion of this study, it was shown that canonical correlation and regression analyses make it possible to utilize many tree-ring chronologies to reconstruct anomalies in climatic variables such as pressure at different seasons and grid points over the Northern Hemisphere. When the number of variables under consideration is large, and when they are likely to be correlated, it is helpful first to reduce the variables of each data set to their orthogonal principal components (eigenvectors).

The amplitudes for the seven eigenvectors of anomalous tree growth which were weighted to give maximum correlation with surface pressure anomalies for all seasons (Fig. 7) may also provide information on other climatic variables correlated with surface pressure. For example, the first author working with C. W. Stockton at the Laboratory of Tree-Ring Research used the amplitudes to predict the annual stream flow of the Colorado River at Lee's Ferry. Variables 1, 4 and 5 were highly significant predictors and accounted for 60% of the variance in stream flow. Thus, it seems plausible that these amplitudes could be used as predictors of such variables as temperature, precipitation, or other climatic variables associated with the regions of high predictability of pressure shown in Fig. 11, but not necessarily associated with any particular trees. The multiple regression weights, **R**, may be estimated for any common calibration period, and the canonically weighted tree-ring chronologies may then be used with the regression weights to reconstruct the particular climatic data for earlier years.

It is recognized that the predictions of individual seasonal pressure anomalies obtained in the preliminary tests are undoubtedly subject to sizable error (Fig. 11). Some failure of prediction could be attributed to the uniformity in the type of tree-ring data used in this preliminary analysis, to the fact that the eigenvectors of tree-ring data used to develop the estimation model were not based on the same period of observation as the corresponding pressure data, to some errors in the tree-ring data which are now corrected, to the choice of grid size and location, and to the arbitrary classification of the four 3-month seasonal periods. Correction of these difficulties will be attempted in future work. A certain portion of the lack of prediction will never be overcome, as tree-ring growth, which is influenced by the climate of previous seasons cannot estimate climatic variation perfectly in any one season.

It is also recognized that there may be a certain amount of nonstationarity and heteroscedasticity (Julian, 1969) in tree-ring and climatic data. However, there is good evidence (LaMarche and Fritts, 1971) that the principal tree-growth anomaly patterns of the present (1931–62) are similar to the anomaly patterns of the past (1700–1930). Also, the sampling replication and the standardizing routines used in compiling the 49 tree-ring chronologies (Fritts, 1969b) give a measure of objectivity and stability as the nonstationarity due to the aging of trees is removed.

Since multivariate analysis is suitable for data diversity, it is now possible to relax to some extent the criteria for extreme selectivity of trees from arid sites (Fritts, 1969b). It appears that one can obtain more information on seasonal variations if a number of ring-width chronologies are used that respond differently to climate throughout each season. The response functions can be utilized to select those chronologies with diverse responses. In future work, selections will also be made for chronology length and the widest geographic coverage in order to obtain a set of chronologies that are continuous back to 1500 A.D. Canonical analyses similar to that described here, as well as canonical regressions, as described by Glahn (1968), are already being made. This latter analysis, which allows use of information about spatial covariance in arriving at the canonical regression weights, has been shown to produce essentially the same results as those described here. Also, we plan to utilize atmospheric pressure for the summer season concurrent with, as well as that preceding, the period of growth. Finally, it may be possible to utilize a network of temperature and precipitation as well as pressure observations (Kutzbach, 1967), in order to more directly relate climatic patterns to tree growth patterns.

We conclude from the preliminary studies that multivariate analysis techniques now make it possible to readily and objectively evaluate the climatic information in ring-width chronologies. This information may be used to make reliable quantitative estimates of climatic or environmental variability, especially that which has occurred over North America and the western sector of the Northern Hemisphere since 1500 A.D.

6. Significance

We believe that the multivariate approaches described herein could revolutionize dendroclimatic analysis. The physiological models are sufficiently adequate that meaningful interpretations will not be difficult to obtain. Well-defined statistical models for the response of trees to their environment can be derived readily, and these can be utilized to study tree growth and environmental relationships, to select tree-ring chronologies, and to structure new dendrochronologic sampling designs. The improved data sets should provide more reliable estimates of past atmospheric circulations and related variables of temperature and precipitation.

The multivariate methods described in the second application, when used on the improved set of ring-width chronologies, are expected to yield a wealth of climatic information which is not only objectively derived, but is dated to the exact year corresponding to the tree rings. Such data will provide a means for studying climatic variability that occurred prior to

existing climatic records. It appears that significant information on pressure patterns over the Pacific Ocean as well as over North America will be obtained (Kutzbach *et al.*)[4]

One approach to the study and evaluation of possible future climates is a study of past climate. A long climatic record can serve to identify the range of possible climates and the characteristics of possible climatic "modes." The work of Lamb (1963, 1969) and Lamb and Johnson (1966) has served to establish estimates of the characteristics of natural climatic variability for the past thousand years. This work, however, is largely restricted to the North Atlantic-European sector and knowledge of climatic variability elsewhere in the Western Hemisphere is less quantitative. Although prediction of climatic changes remains a task for the future, some estimates of "possible" climates would be useful for planning purposes. Furthermore, as sophistication in the modeling of present climate is achieved (e.g., Manabe *et al.*, 1970), it becomes essential that accurate maps of past climatic patterns be available for making comparisons (Sheppard, 1966). Finally, the need for a clearer understanding of "natural" modes of climatic variability is enhanced by recent hypotheses regarding man's inadvertent role in changing climate. That is, knowledge of past climatic variability may help to discriminate between "natural" and "man-produced" or "man-accentuated" changes.

More specifically, several questions require answers.

1) What are the climatic modes of the recent past (1500–1970)?

2) What are some of the essential characteristics of recent climatic modes?

3) Are the climatic modes coincident with man's activities unique or is there historical evidence for their past occurrence?

Initial dendroclimatic work using multivariate techniques shows considerable potential in offering the data input needed to answer these questions.

In the future more well-dated tree-ring chronologies and other well-dated proxy series of climate will undoubtedly become available from other sectors of the Northern and Southern Hemispheres. The same techniques can be utilized to transform the information from diverse proxy series into estimates of anomalies in pressure. Such estimates from an enlarged set of proxy series may allow the reconstruction of global variations in the world's circulation and could provide an extended, worldwide estimate of year-by-year climatic variability and change.

Acknowledgments. This research was supported at the University of Arizona by NOAA Grants E-231-68(G) and E-41-70(N), and in late stages by NSF Grant GA-2658. Portions of the work carried on at the University of Wisconsin were supported by NSF Grant GA-10651X. The general model was conceived while the senior author was a John Simon Guggenheim Fellow in 1968–69 at the University of Wisconsin. Terence J. Blasing contributed a large part of the statistical descriptions, made some of the computations for the response functions and canonical regression, and verified the predictions with the data of Lamb.

Bruce P. Hayden helped in designing the experiment and performing analyses of the pressure anomalies. John E. Kutzbach provided valuable counsel and direction for the paleoclimatic analysis and for the section on "Significance." The authors wish to express appreciation to J. Murray Mitchell, Jr., Reid A. Bryson, William D. Sellers and Hubert H. Lamb for their interest and their encouragement of the research and to A. K. Gupta and P. K. Bhattacharya, who contributed in resolving some problems in the mathematical techniques.

[4] Kutzbach, J. E., B. P. Hayden and T. J. Blasing, 1970: Diagnostic study of present circulation variability and inferred circulation variability since 1000 A.D. Unpublished manuscript.

REFERENCES

Bryson, R. A., and J. F. Lahey, 1958: The march of the seasons. University of Wisconsin, Final Rept., Contract AF 19-(604)-992, 41 pp.

Draper, N. R., and H. Smith, 1966: *Applied Regression Analysis.* New York, Wiley, 407 pp.

Fritts, H. C., 1962: An approach to dendroclimatology: Screening by means of multiple regression techniques. *J. Geophys. Res.*, **67**, 1413–1420.

——, 1963: Computer programs for tree-ring research. *Tree-Ring Bull.*, **25**, 2–7.

——, 1965: Tree-ring evidence for climatic changes in western North America. *Mon. Wea. Rev.*, **93**, 421–443.

——, 1969a: *Bristlecone Pine in the White Mountains of California: Growth and Ring-Width Characteristics.* Tucson, University of Arizona Press, 44 pp.

——, 1969b: Tree-ring analysis: A tool for water resources research. *Trans. Amer. Geophys. Union*, **50**, 22–29.

——, 1970: Tree-ring analysis and reconstruction of past environments. Vancouver, *University of British Columbia Faculty of Forestry*, Bull. No. 7, 92–98.

——, D. G. Smith and M. A. Stokes, 1965a: The biological model for paleoclimatic interpretation of Mesa Verde tree-ring series. *Mem. Soc. Amer. Archeol.*, **19**, 101–121.

——, ——, J. W. Cardis and C. A. Budelsky, 1965b: Tree-ring characteristics along a vegetation gradient in northern Arizona. *Ecology*, **46**, 393–401.

——, J. E. Mosimann and C. P. Bottorff, 1969: A revised computer program for standardizing tree-ring series. *Tree-Ring Bull.*, **29**, 15–20.

Glahn, H. R., 1968: Canonical correlation and its relationship to discriminant analysis and multiple regression. *J. Atmos. Sci.*, **25**, 23–31.

Glock, W. S., E. M. Gaines and S. R. Agerter, 1964: Soil-moisture fluctuations under two ponderosa pine stands in northern Arizona. U. S. Forest Service, Res. Paper RM-9.

——, and S. R. Agerter, 1969: Tree growth and precipitation near Flagstaff, Arizona. *Yearbook of the Association of Pacific Coast Geographers*, Vol. 30, Corvallis, Oregon State University Press, 79–106.

Kutzbach, J. E., 1967: Empirical eigenvectors of sea-level pressure, surface temperature and precipitation complexes over North America. *J. Appl. Meteor.*, **6**, 791–802.

——, 1970: Large-scale features of monthly mean Northern Hemisphere anomaly maps of sea-level pressure. *Mon. Wea. Rev.*, **98**, 708–716.

Julian, P. R., 1969: An application of rank-order statistics to the joint spacial and temporal variations of meteorological elements. *Mon. Wea. Rev.*, **98**, 142–153.

——, and H. C. Fritts, 1968: On the possibility of quantitatively extending climatic records by means of dendroclimatological analysis. *Preprints of Papers, First Statist. Meteor. Conf.*, Hartford, Conn., Amer. Meteor. Soc., 76–82.

LaMarche, V. C., Jr., and H. C. Fritts, 1971: Anomaly patterns of climate over western United States, 1700–1930, derived from principal component analysis of tree-ring data. *Mon. Wea. Rev.*, **99**, 138–142.

Lamb, H. H., 1963: On the nature of certain climatic epochs which differed from the modern (1900–1939) normal. *Changes of Climate*, UNESCO Arid Zone Research Series XX, 125–150.

——, 1969: The new look of climatology. *Nature*, **223**, 1209–1215.

——, and A. I. Johnson, 1966: Secular variations of the atmospheric circulation since 1750. *Geophys. Mem.* No. 110, Meteorological Office, London, 125 pp.

Manabe, S., J. Smogorinsky, J. L. Holloway, Jr., and H. M. Stone, 1970: Simulated climatology of a general circulation model with a hydrologic cycle: III. Effects of increased horizontal computational resolution. *Mon. Wea. Rev.*, **98**,172–212.

Mintz, Y., 1968: Very long-term global integration of the primitive equations of atmospheric motion: An experiment in climatic simulation. *Meteor. Monogr.*, **8**, No. 30, 20–36.

Sellers, W. D., 1968: Climatology of monthly precipitation patterns in the western United States, 1931–1966. *Mon. Wea. Rev.*, **96**, 585–595.

Sheppard, P. A., 1966. Preface. *World Climate from 8000 to 0 B.C.*, London, Royal Meteorological Society, p. 1.

Stokes, M. A., and T. L. Smiley, 1968: *An Introduction to Tree-Ring Dating*. University of Chicago Press, 73 pp.

U. S. Weather Bureau, 1961, 1962: *Climatological Data*. Asheville, N. C., U. S. Dept. Commerce, 48, 49, No. 1–13.

——, 1963: Decennial census of United States climate, monthly averages for state climatic divisions, 1931–1960. *Climatography of the United States*, No. 85, Washington, D. C.